

Refining Feature Embedding with Semantic-Aligned Attention for Few-Shot Classification

Xianda Xu, Xing Xu, Jiwei Wei, Fumin Shen, Yang Yang and Heng Tao Shen

Abstract—Few-shot classification aims to recognize unseen images from new classes given a limited number of labeled images in each new class. Successful embedding and metric-learning approaches to this task normally learn a feature comparison framework between an unseen image and the labeled images. However, these approaches usually have problems with ambiguous feature embedding because they tend to ignore important local visual and semantic information when extracting intra-class common features from the images. In this paper, we introduce a Semantic-Aligned Attention (SAA) mechanism to refine feature embedding and it can be applied to most of the existing embedding and metric-learning approaches. The mechanism highlights pivotal local visual information with attention mechanism and aligns the attentive map with semantic information to refine the extracted features. Incorporating the proposed mechanism into the prototypical network, evaluation results reveal competitive improvements in few-shot classification on both miniImageNet and tieredImageNet benchmark datasets. We further extend the proposed mechanism to zero-shot classification and consistently achieve promising performance on both CUB and SUN datasets.

Index Terms—few-shot classification, zero-shot classification, attention mechanism, visual-semantic alignment

I. INTRODUCTION

Deep neural networks have achieved remarkable results in visual recognition tasks [1], [2], [3]. However, these conventional methods usually require large-scale datasets such as ImageNet [4]. It severely adds burden to the cost of collecting data and limits their adaptability to new classes with rare examples. Driven by the defects of the conventional deep learning methods, more and more attention has been drawn to *few-shot classification* [5].

Few-shot classification aims to recognize new classes with little supervised data. Specifically, it classifies unseen images into a set of new classes with a limited number of labeled images in each new class. The shortage of labeled data lead to overfitting and generalization issues in conventional deep learning methods so new approaches to this problem are being studied. The data augmentation approaches [6], [7], [8], [9], [10] alleviate overfitting by expanding the training dataset to meet the sufficient sample complexity, but they do not solve the problem in essence. The optimization approaches [11], [12], [13], [14], [15], [16], [17] learn to fine-tune the model from an abundant-data regime, but they are affected

X. Xu, X. Xu, J. W, Y. Yang, F. Shen and H. T. Shen are with the Center for Future Multimedia and School of Computer Science and Engineering, University of Electronic Science and Technology of China, Chengdu 610051, China (Email: bryce_xu@163.com, xing.xu@uestc.edu.cn, mathe-matic6@gmail.com, dlyang@gmail.com, fumin.shen@gmail.com, shenheng-tao@hotmail.com)

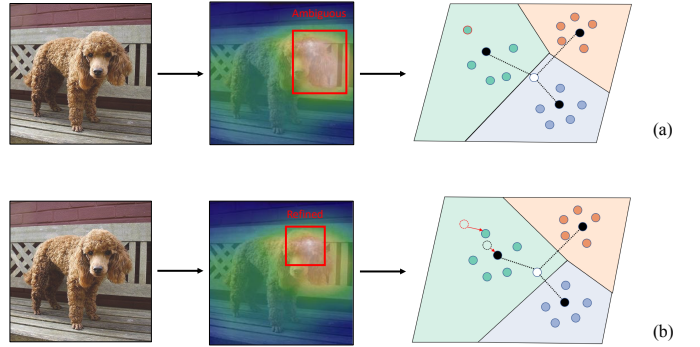


Fig. 1. Labeled images in each class are mapped into a common embedding space to generate class embeddings (black dots). The feature embedding of one test image (white dot) is categorized by measuring its distance to each class embedding. (a) Noisy global distraction brought by ambiguous feature embedding in most metric-learning approaches might lead to a failure in class embedding. (b) Refined local feature embedding with the proposed Semantic-Aligned Attention (SAA) mechanism helps find intra-class commonality and cluster support embeddings more firmly.

by previous tasks without checking the relatedness of the two tasks. Therefore, a recent increase of interest emerges in the embedding and metric-learning approaches.

The embedding and metric-learning approaches [18], [19], [20], [21], [22], [23] produce feature embeddings for comparison between each unlabeled sample embedding and the class embeddings [18]. Specifically, they roughly follow three steps: (1) using a feature embedding network to map all the labeled (support) and unlabeled (query) samples into an embedding space; (2) representing each class in the embedding space based on the embeddings of its support samples; (3) measuring the distances of each query sample embedding to all the class embeddings and assigning each query sample to the nearest class. The first step, also known as feature embedding, is decisive in class embedding. To alleviate overfitting, most embedding and metric-learning approaches [20], [21], [22] adopt a simple 4-layer convolutional network in feature embedding, which suffers from the following two major limitations.

The first limitation is that the feature embedding and measuring network tends to extract global features, which makes it prone to bring noisy information such as background distraction. Fig. 1(a) describes the failure that ambiguous feature embedding may lead to in class embedding [24]. The advantage of local features here is that they reflect intra-class commonality much better, which further makes class embedding more distinctive from each other.

The second limitation is that the feature embedding and measuring network ignores the use of semantic information.

When human beings recognize an object, they not only focus on visual information but also consider some prior knowledge like semantic descriptions of the object. It indicates that there is a latent correlation between visual information and the semantic knowledge in human's brain [25], [26]. Semantic information accessible to few-shot classification is usually the label embeddings learned from large unsupervised text corpora [27]. Exploring the relationship between visual information and the semantic knowledge could assist the process of feature embedding and class embedding [28], [29].

Motivated by the two limitations in the existing feature embedding network, we propose a semantic-aligned attention (SAA) mechanism for few-shot classification. Specifically, we leverage the attention mechanism to highlight pivotal local information and alleviate noisy global distraction. We learn the visual-and-semantic correlation and align the visual attentive maps with it to further refine the extracted local features. Our method can be applied to most embedding and metric-learning approaches and further improve performance. Fig. 1(b) shows how refined local feature embedding in our approach could help find the intra-class commonality and improve class embedding.

We further extend our method to zero-shot classification. Rather than a few labeled examples in few-shot classification, each new class in zero-shot classification comes with side information, usually attribute vectors. Like we do in few-shot classification, we improve class embedding in zero-shot classification by incorporating the class label embeddings into the network.

To sum up, our contributions in this work include:

- We introduce a semantic-aligned attention (SAA) mechanism for few-shot classification to refine feature embedding. The mechanism refines feature embedding with important local visual information aligned with semantic information to improve class embedding.
- We extend our method to zero-shot classification. The network improves class embedding by absorbing knowledge from a semantic vector concatenated with attributes and label embeddings.
- Experimental results show that our method brings a considerable performance boost to the existing embedding and metric-learning approaches such as the prototypical network in both few-shot classification and zero-shot classification.

The remainder of the paper is organized as follows. In Section 2, we review about the related work in few-shot classification and zero-shot classification respectively. Section 3 contains the elaboration of the proposed approach. We present extensive experimental studies on few-shot classification and zero-shot classification in Section 4. The conclusion is drawn in Section 5.

II. RELATED WORK

In this section, we conduct a review of the related work in few-shot learning and zero-shot learning. We begin by introducing three paradigms in few-shot learning. Next, we discuss the research progress in zero-shot learning.

Few-shot Learning: Much attention has been drawn to this task in recent years. Existing approaches to few-shot learning

can be roughly divided into three paradigms: (i) data augmentation (ii) optimization (iii) embedding and metric-learning.

Data augmentation approaches [6], [7], [8], [9], [10] are straightforward as they solve the few-shot learning task by augmenting the number of labeled samples in each novel class. One category focus on transforming existing datasets. The idea in the early works is to copy original samples and modify the new samples with learned transformation. Schwartz *et al.* [9] applies auto-encoders that add the new samples with the intra-class variances learned from a similar class, while Hariharan *et al.* [8] assumes general transformable variability among all categories and hallucinates novel-class samples with a set of learned transformation functions from base-class samples. In recent works, Tsutsui *et al.* [10] generates new samples with GANs and learns to synthesize them with original samples. Chen *et al.* [7] trains an image deformation sub-network to produce additional novel-class samples. The other category explores to transform external datasets. For example, Chen *et al.* [6] combines blocks from the existing labeled images and the unlabeled gallery images in a self-training scheme.

Optimization approaches [11], [12], [13], [14], [15], [16], [17] meta-learn an algorithm to fine-tune the model in the case of few-shot learning. In early works, Finn *et al.* [11] proposes MAML that learns a good initialization so that the classifiers for novel classes can be learned with a small number of gradient update steps. Li *et al.* [13] presents Meta-SGD which learns a good optimizer for the new task. Ravi *et al.* [16] designs an LSTM-based meta-learner that learns both the initialization and the optimizer. These methods have been improved in recent years. Based on MAML, Jamal *et al.* [12] presents an entropy-based meta-learning approach to alleviate the bias towards existing tasks in the initial model and Nichol *et al.* [15] introduces first-order optimization to save computation. Mishra *et al.* [14] and Sun *et al.* [17] both study the failure of adopting deep neural networks for few-shot learning tasks and they tackle by meta-learning a set of scaling and shifting functions.

Embedding and metric-learning approaches train a neural network to embed all the labeled and unlabeled samples into an embedding space so that the similar pairs and dissimilar pairs can be identified using a metric. Inductive embedding and metric-learning approaches [20], [21], [22] are traditional and only support samples are used in the model training. Based on [22], the prototypical network [20] uses the mean of support embeddings as the class representation (or the prototype) and the Euclidean distance as the metric. The relation network [21] further learns the metric by evaluating each query-support pair with a neural network. Transductive embedding and metric-learning approaches [19], [23] are less ambitious and the entire query set is also involved in the model training. For example, Oreshkin *et al.* [19] learns a task-dependent metric and Ye *et al.* [23] learns the adaptation of embeddings to each task.

Our work improves inductive embedding and metric-learning approaches by introducing a semantic-aligned attention mechanism. Before our work, several networks with attention mechanism [30], [31], [32], [33], [34], [24] have achieved good results in few-shot classification. Task-dependent attention networks are presented in [32][24] and [34], but they

are transductive approaches and not as universal as inductive approaches. Inductive approaches like [30] and [33] localize relevant regions with visual information but without the help of semantic information. Hao et al.'s work [31] is related to ours. But their work is based on the relation network [21] and semantic alignment is used to select attentive region pairs instead of semantically guiding visual attention in the embedding network to better focus on regional intra-class commonality.

Zero-shot Learning: Our method is designed for few-shot learning, but it can be elegantly extended to zero-shot learning. Like few-shot learning, zero-shot learning aims to recognize new classes whose instances are not seen during training. But in zero-shot learning, each new class comes with side information, usually semantic knowledge, rather than a few labeled samples.

Early works in zero-shot learning [35], [36], [37], [38], [39] directly learn a mapping from an image feature space to a semantic space. For example, Akata *et al.* [35] learn a bilinear compatibility function between the image feature space and the semantic space using ranking loss. The compatibility function is further optimized by [36] with SVM loss and [39] with a regularizer. Bucher *et al.* [37] improve the consistency of the semantic embedding with metric-learning in the semantic space.

Recent advances [20], [40], [41], [42], [43], [44], [45] focus on learning deep multi-modal embeddings. Socher *et al.* [44] use a two-layer neural network to project image features into a semantic space. Zheng *et al.* [45] argue that the image feature space is more discriminative so they map semantic features into the image feature space instead with a deep embedding model. Reed *et al.* [41] learn deep multi-modal embeddings for both image features and semantic knowledge, which is further improved in the following works [20], [40], [42], [43].

Our work uses a deep neural network to generate both image feature embeddings and semantic embeddings. Following [20], we obtain class embeddings by transforming the semantic attribute vectors in each class. We improve the process by introducing semantic-alignment to the transformation network and we again benefit from gaining additional semantic knowledge.

III. THE PROPOSED APPROACH

This section presents our proposed approach to dealing with few-shot classification and zero-shot classification. We begin by offering a problem definition of few-shot classification and zero-shot classification. Next, we introduce our Semantic-Aligned Attention (SAA) mechanism and show how our method is implemented in the feature embedding network of few-shot classification. At last, we extend our work to zero-shot classification and demonstrate how to improve the task with the label embeddings.

A. Problem Definition

Few-shot classification deals with a supervised learning task given a dataset $D = \{D^{\text{train}}, D^{\text{val}}, D^{\text{test}}\}$ which consists of a training set, a validation set and a test set. The three

sub-datasets have different label spaces, which means that a certain class in one of the three sub-datasets is unseen in the other two sub-datasets.

In traditional classification, the three sub-datasets share the same label space and each class has a massive number of samples. That is why we could easily train a classifier to assign a class to each sample in the test set. However, since the three sub-datasets in few-shot classification are disjoint with each other and each class is given a few number of samples, such a classifier does not work well in such a circumstance. Therefore, meta-learning is normally performed on the training set, in order to learn transferrable knowledge about how to classify from N new classes with K examples in each class. It allows us to perform better few-shot classification on the test set.

Most successful few-shot classification approaches follow an *Episodic Training* paradigm proposed by [22] which simulates the few-shot classification task during training. Under this paradigm, a N -way K -shot *episode* contains two sets: (1) the *support* set $\mathcal{S} = \{(s_i, y_i)\}_{i=1}^{N \times K}$ with K samples from each of the N classes (2) the *query* set $\mathcal{Q} = \{(q_j, y_j)\}_{j=1}^{N \times Q}$ with Q samples from each of the N classes. The *support* set and the *query* set are disjoint ($S \cap Q = \emptyset$) with each other. A certain image can never co-exist in both sets. All the training, validation and test processes are implemented on *episodes* which are randomly sampled from each dataset. In each training iteration, the model is updated in an *episode* and in each validation or test iteration, one *episode* is validated or tested.

Zero-shot classification is similar to few-shot classification but with K kept to 0, which means labeled samples are not available to each test class. Instead, each class comes with side information, usually class attribute vectors $V = \{v_k\}_{k=1}^N$ describing the semantic attributes of each class. $X = \{(x_m, y_m)\}_{m=1}^{N \times M}$ is the set of samples with M samples from each of the N classes. Since the three sub-datasets are disjoint with each other, meta-learning is also performed on the training set.

B. Semantic-Aligned Attention (SAA) Mechanism

The Semantic-Aligned Attention (SAA) mechanism is illustrated in Fig. 2, which consists of two branches, i.e., the Spatial Attention Mechanism and the Semantic Alignment Mechanism. The first branch is to extract more important local features. The second branch is to align the local features with semantic information. It generates a semantic-aligned attentive map $M_r \in \mathbf{R}^{1 \times H \times W}$ based on the input feature map $F \in \mathbf{R}^{C \times H \times W}$. The output feature map $F' \in \mathbf{R}^{C \times H \times W}$ would be:

$$\mathbf{F}' = \mathbf{F} \otimes \mathbf{M}_r. \quad (1)$$

where \otimes is element-wise multiplication. Through multiplication, the attention values can be broadcasted accordingly.

1) Spatial Attention Mechanism:

Inspired by [46], [47], the spatial attention mechanism in our method is designed to explore the inter-spatial relationship

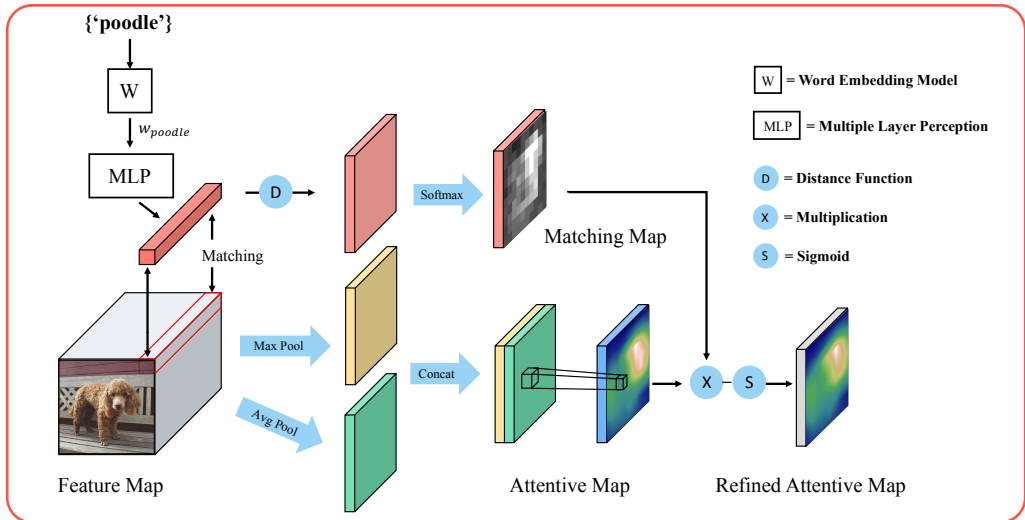


Fig. 2. The overall architecture of our Semantic-Aligned Attention (SAA) mechanism. It generates an visual attentive map with the spatial attention mechanism and a visual-semantic matching map with the semantic alignment mechanism. The refined visual attentive map is produced by combining and then activating these two maps.

of features in the input feature map. In other words, it helps decide “where” to focus on in the feature map.

Specifically, the spatial attention mechanism firstly applies average-pooling and max-pooling operations along the channel dimension to generate the following two visual maps: $F_{avg} \in \mathbf{R}^{1 \times H \times W}$ and $F_{max} \in \mathbf{R}^{1 \times H \times W}$. Then, it concatenates these two visual maps and obtains the attentive map $M_a \in \mathbf{R}^{1 \times H \times W}$ by applying a convolution operation on the concatenated visual map to determine where to emphasize or suppress. To sum up, M_a is obtained as:

$$\begin{aligned} M_a &= Conv([f_{ap}(\mathbf{F}); f_{mp}(\mathbf{F})]) \\ &= Conv([\mathbf{F}_{avg}; \mathbf{F}_{max}]). \end{aligned} \quad (2)$$

where f_{ap} is the average-pooling operation, f_{mp} is the max-pooling operation and $Conv$ is the convolution operation with the filter size of 7×7 in our few-shot classification experiments.

2) Semantic Alignment Mechanism:

The semantic alignment mechanism in our method is used to associate visual local regions with class label embeddings. By exploring the relationship between visual information and the pre-learned semantic knowledge (the label embeddings), it helps locate informative visual region and refine the visual attentive map. Note that it is only applied in feature embedding of the support samples since the label embeddings are not accessible to query samples.

We obtain the label embeddings of all the classes in each set using a word embedding model W , which is *GloVe* [27] in this work. The word embedding model is pre-trained on large text corpora and could offer valuable prior knowledge. The label embeddings are then transformed via a multiple layer perceptron [48] to match the channel dimension of the input feature map.

Each episode contains N label embeddings belonging to N different classes and for each support sample, it has 1 positive label embedding w^+ and $N - 1$ negative label embeddings $\{w_n^-\}_{n=1}^{N-1}$. A visual-semantic matching map M_w can be generated using w^+ based on the input feature map with M_{wi} representing the relevance between w^+ and the local region F_i :

$$M_{wi} = \frac{\exp(f_s(w^+, F_i))}{\sum_j \exp(f_s(w^+, F_j))}. \quad (3)$$

where f_s is the similarity function measuring the relevance between two embeddings.

Therefore, the refined attentive map M_r can be achieved by multiplying the attentive map and the matching map and then activating with the sigmoid function [49]:

$$M_r = \sigma(M_w \otimes M_a). \quad (4)$$

In order to link visual local regions and class label embeddings, $loss_w$ is introduced here. The loss function is inspired

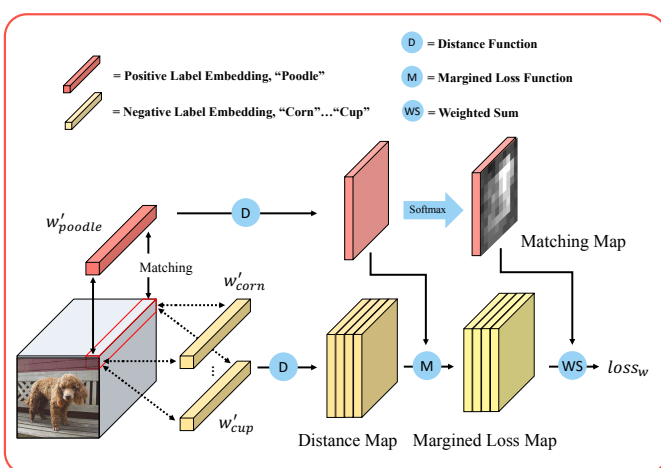


Fig. 3. The illustration of computing $loss_w$ in the 5-way scenario. In this case, the positive class is “Poodle” and the rest four classes are negative classes.

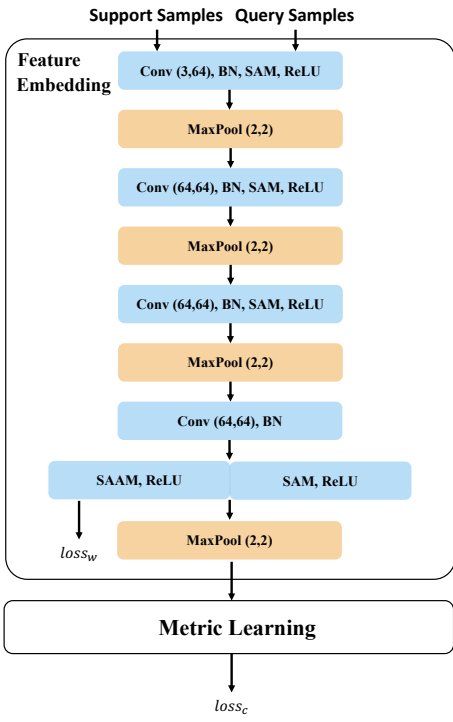


Fig. 4. The architecture of the feature embedding neural network in few-shot classification. It chooses *ConvNet* as the basic feature embedding network.

from [38], [50]. $loss_w$ needs to be computed in each episode, which is:

$$loss_w = \sum_{n=1}^{N-1} \sum_{\mathbf{F}_i \in \mathbf{F}} \left[\mathbf{M}_{wi} \cdot |\alpha + f_s(\mathbf{w}_n^-, \mathbf{F}_i) - f_s(\mathbf{w}^+, \mathbf{F}_i)|_+ \right]. \quad (5)$$

where α is a manually-set margin and M_{wi} here is for reinforcing the relevance between w^+ and F_i . Fig. 3 well illustrates the computing process of $loss_w$ in one episode.

C. Network Architecture

Following most existing embedding and metric-learning approaches, we choose *ConvNet* as the neural network architecture for feature embedding in few-shot classification, as shown in Fig. 4.

The neural network consists of four convolutional blocks. The first three blocks contain a convolution layer with $64 \times 3 \times 3$ filters, a batch normalization layer, a spatial attention mechanism layer and a ReLU nonlinearity layer. The last block replaces the spatial attention mechanism layer with the semantic-aligned attention mechanism layer for the support samples while keeps the same for the query samples. A 2×2 max-pooling layer is placed between every two convolutional blocks. The output size of the feature embedding network is $D = 64 * 5 * 5 = 1600$ for both the miniImageNet dataset and the tieredImageNet dataset.

The neural network generates 1600-dimensional feature embeddings of both the support samples and the query samples in the episode, which are used in the following metric-learning process. The support feature embeddings are utilized

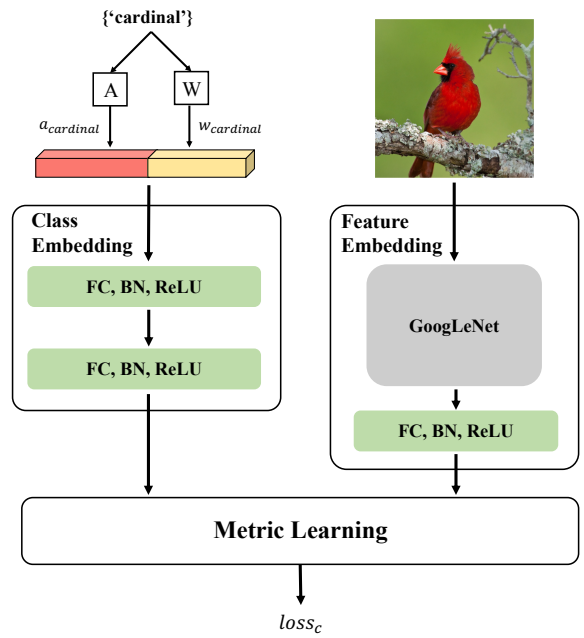


Fig. 5. The architectures of the class embedding neural network and the feature embedding neural network in zero-shot classification

to form class embeddings and the query feature embeddings are measured to every class embedding to determine which class they belong to.

There are two losses in the whole workflow. One is $loss_w$ used to update the visual-semantic network in the semantic alignment mechanism. The other one is $loss_c$ (seen in equation 9) used to update the overall network. A hyper-parameter λ is introduced in calculating the overall network loss. Therefore, the network loss would be:

$$loss = loss_c + \lambda \cdot loss_w. \quad (6)$$

D. Zero-shot Classification

Zero-shot classification differs from few-shot classification in that it produces class embeddings based on side information rather than feature embeddings from labeled samples. Most embedding and metric-learning approaches choose class attribute vectors as side information. These vectors are usually provided by the dataset, describing semantic attributes of each class in the dataset. Here, like our approach in few-shot classification, we improve class embedding by introducing additional semantic information, the class label embeddings to the network. We achieve so by concatenating the class attribute vectors and the class label embedding and then sending the concatenated vector to the following class embedding network.

We follow the architectures of the class embedding neural network and the feature embedding neural network in most embedding and metric-learning approaches to zero-shot classification, as shown in Fig. 5.

The class embedding network learns a linear network to create a 1024-dimensional embedding space. Each linear block consists of a fully-connected layer, a batch normalization layer and a ReLU nonlinearity layer. We use the default class

attribute vectors offered in the dataset and obtain the class label embeddings using *GloVe* like in few-shot classification.

The feature embedding network utilizes a pre-trained GoogLeNet [3] as the main feature embedding model. In order to match the dimension of the embedding space, we replace its last linear block with a new linear block so that the output size of the feature embedding network can be reshaped to 1024.

During the process of metric learning, the feature embedding of each sample is measured to the class embeddings in the embedding space and then assigned to the nearest one. $loss_c$ is used to update the overall network.

IV. EXPERIMENTS

We test our approach on one effective embedding and metric-learning approach, namely the prototypical network [20]. In the few-shot classification task, the improved prototypical network is evaluated on the two widely used datasets: the miniImageNet dataset [22] and the tieredImageNet dataset [51]. In the zero-shot classification task, the improved prototypical network is evaluated on the CUB dataset [52] and the SUN dataset [53]. All the experiments are implemented using the PyTorch framework [54].

A. Prototypical Network

In this paper, we evaluate our approach on the prototypical network [20]. As a matter of fact, our approach is plug-and-play for most existing embedding and metric-learning approaches. We choose the prototypical network in this paper due to its simplicity.

1) Few-shot Classification:

During the process of feature embedding, the prototypical network maps all the support samples and the query samples into a D -dimensional embedding space using the feature embedding neural network. The feature embedding neural network $f : \mathbb{R}^V \rightarrow \mathbb{R}^D$, parameterized by θ_f , is used to learn the embedding space where samples of the same class are clustered closely and samples of different classes are separated widely.

Then, during the process of metric learning, the prototypical network firstly computes the class embedding (or the prototype) for each class in the current episode by averaging its support embeddings. For example, the prototype of class c is computed as:

$$\mathbf{p}_c = \frac{1}{|S_c|} \sum_{(s_i, y_i) \in S_c} f(\mathbf{s}_i). \quad (7)$$

Next, the prototypical network produces a distribution over the N classes within the episode for each query feature embedding $f(q_j)$ based on a softmax over the Euclidean distances to the class embeddings (or the prototypes) in the embedding space:

$$\mathbf{p}(y = c | q_j) = \frac{\exp(-d(f(\mathbf{q}_j), \mathbf{p}_c))}{\sum_{c'} \exp(-d(f(\mathbf{q}_j), \mathbf{p}_{c'}))). \quad (8)$$

In each training iteration, the loss used to update the feature embedding neural network is calculated as:

$$loss_c = \sum_{c=1}^N \sum_{j=1}^Q \left[d(f(\mathbf{q}_j), \mathbf{p}_c) + \log \sum_{c'} \exp(-d(f(\mathbf{q}_j), \mathbf{p}_{c'})) \right]. \quad (9)$$

2) Zero-shot Classification:

The class embedding process in zero-shot classification maps the class attribute vectors into a D' -dimensional embedding space via the class embedding neural network $g : \mathbb{R}^A \rightarrow \mathbb{R}^{D'}$ parameterized by θ_g . For example, the prototype of class c is computed as:

$$\mathbf{p}_c = g(\mathbf{v}_k). \quad (10)$$

Meanwhile, the feature embedding process produces the feature embedding of each sample x_m using the pre-trained deep neural network $f' : \mathbb{R}^{V'} \rightarrow \mathbb{R}^{D'}$. The distance-based distribution for each sample x_m over the N classes and the computation of $loss_c$ follow the equation 8 and the equation 9 respectively.

B. Datasets

The few-shot classification task is evaluated on the miniImageNet dataset and the tieredImageNet dataset while the zero-shot classification task is tested on the CUB dataset and the SUN dataset.

The miniImageNet dataset [22] is actually a subset of the ImageNet-2012 dataset [55], which consists of 100 classes with 600 images in each class. We follow the standard splitting rule given by Vinyals *et al.* [22]: 64 classes for training, 16 classes for validation and 20 classes for testing.

The tieredImageNet dataset [51] is also but a larger subset of the ImageNet-2012 dataset [55], which comprises totally 608 classes. Following the standard splitting rule provided by Ren *et al.* [51], we manage the dataset in the following way: 351 classes for training, 97 classes for validation and 160 classes for testing.

The CUB dataset [52] is a fine-grained image dataset which contains 11,788 images of 200 bird classes. Each class is annotated with 312 attributes encoding characteristics like color and shape. Following the splitting rule provided by Snell *et al.* [20], we divide the classes into: 100 classes for training, 50 classes for validation and 50 classes for testing.

The SUN dataset [53] is also a fine-grained image dataset which consists of 14340 images of 717 types of scenes. Each class is annotated with 102 attributes. Following [56], we use 645 classes for training (65 classes randomly selected for validation) and 72 classes for testing.

C. Implementation Details

Few-shot classification experiments are implemented on 5-way 1-shot and 5-way 5-shot settings. The input image size is 84×84 and no data augmentation is involved during training. The model is trained for 120 epochs, with 4 episodes in each mini-batch and 200 mini-batches in each epoch. We use Adam

[57] as the optimizer with an initial learning rate of 10^{-3} and a weight decay of 5×10^{-5} . For the miniImageNet dataset, the learning rate is dropped by half every 12,000 episodes. For the tieredImageNet dataset, the learning rate is dropped by half every 18,000 episodes. We use *GloVe* [27] as the pre-trained word embedding model and generate all the label embeddings from it. Each label embedding has a length of 300 in dimension. The manually-set margin α in computing $loss_w$ is set to be 0.3 in the 5-way 1-shot setting and 0.4 in the 5-way 5-shot setting. The hyper-parameter λ in the overall network loss is set to be 1.0. The overall accuracy is counted as the average testing accuracy of the 16,000 episodes sampled from the testing set. Each episode contains 15 query images for each class in all the training, validation and test procedures. The number of query images in each episode is constrained by the GPU memory.

Zero-shot classification experiments are implemented on the two datasets. The input image is resized to 256×256 and there is no data augmentation during training. The feature embedding network generates and reshapes the features to 1024 dimensions. A linear class embedding network produces the 1024-dimentional prototypes in the embedding space based on the concatenated vectors between the class attribute vectors and the class label embeddings. The prototypes are formalized to the unit length. The class attribute vectors provided by the datasets are 312-dimentional in the CUB dataset and are 102-dimentional in the SUN dataset. The class label embeddings generated with the pre-trained word embedding model *GloVe* [27] are 300-dimentional during the CUB experiment and are 100-dimentional during the SUN experiment. For both datasets, the networks are trained for 50 epochs, with 10 episodes in each epoch. We use Adam [57] as the optimizer with an initial learning rate of 10^{-4} with a weight decay of 10^{-5} . Each episode contains 5 query images for each class, which is also constrained by the GPU memory.

D. Results

1) *Few-shot Classification*: In few-shot classification, we evaluate our proposed approach on the prototypical network and we compare the improved version with other existing methods on the miniImageNet dataset shown in Table I and the tieredImageNet dataset shown in Table II.

For fair comparisons, all the methods in the table have the following common ground: (i) data augmentation is not involved during training; (ii) basic feature embedding network is the *ConvNet*; (iii) they are all inductive methods. They can roughly divided into three categories. As shown in Table I, the first block of the methods are memory-based methods, the second are optimization-based methods and the last are embedding and metric-learning methods.

It is easy to observe the effectiveness of our SAA approach. With SAA, the improved version of the prototypical network performs much better in few-shot classification on both of the datasets. For example, under the 5-way 5-shot setting, the performance is 68.20% v.s. 70.86%, and 72.69% v.s. 74.28% on the miniImageNet dataset and the tieredImageNet dataset respectively. Furthermore, it compares favorably against most

TABLE I
FEW-SHOT CLASSIFICATION ACCURACIES ON THE MINIIMAGENET DATASET. “~” MEANS “NO REPORTED”. ALL THE INCLUDED APPROACHES USE *ConvNet* AS THE BASIC FEATURE EMBEDDING NETWORK.

Paradigm	Model	5-way 1-shot	5-way 5-shot
Memory-based	MetaNet [58]	49.21 ± 0.96	~
	MM-Net [59]	53.57 ± 0.48	66.97 ± 0.35
Optimization-based	MAML [11]	48.70 ± 1.84	63.11 ± 0.92
	Meta-SGD [13]	50.47 ± 1.87	64.03 ± 0.94
	REPTILE [15]	49.97 ± 0.32	65.99 ± 0.58
	MAML++ [60]	52.15 ± 0.26	68.32 ± 0.44
Embedding-and-metric-learning-based	MatchingNet [22]	43.44 ± 0.77	60.60 ± 0.71
	Subspace [61]	~	68.12 ± 0.67
	ProtoNet [20]	49.42 ± 0.78	68.20 ± 0.66
	RelationNet [21]	50.44 ± 0.82	65.32 ± 0.70
Our Method		53.18 ± 0.74	70.86 ± 0.69

TABLE II
FEW-SHOT CLASSIFICATION ACCURACIES ON THE TIEREDIMAGENET DATASET. “~” MEANS “NO REPORTED”. ALL THE INCLUDED APPROACHES USE *ConvNet* AS THE BASIC FEATURE EMBEDDING NETWORK.

Paradigm	Model	5-way 1-shot	5-way 5-shot
Optimization-based	MAML [11]	49.0 ± 1.8	66.5 ± 0.9
	MAML++ [60]	51.5 ± 0.5	70.6 ± 0.5
Embedding-and-metric-learning-based	Soft k-means [51]	52.39 ± 0.44	69.88 ± 0.20
	Subspace [61]	~	71.15 ± 0.67
	ProtoNet [20]	53.31 ± 0.89	72.69 ± 0.74
	RelationNet [21]	54.48 ± 0.93	71.32 ± 0.78
Our Method		56.04 ± 0.83	74.28 ± 0.72

of the other methods coming from the three categories by a large margin.

We also compare the validation accuracy between the networks with our method and the networks without our method on the miniImageNet dataset, as shown in Fig. 6. It shows a faster convergence in our method under both settings of 5-way 1-shot and 5-way 5-shot. We believe that this is because our method could find a better class embedding in a short time.

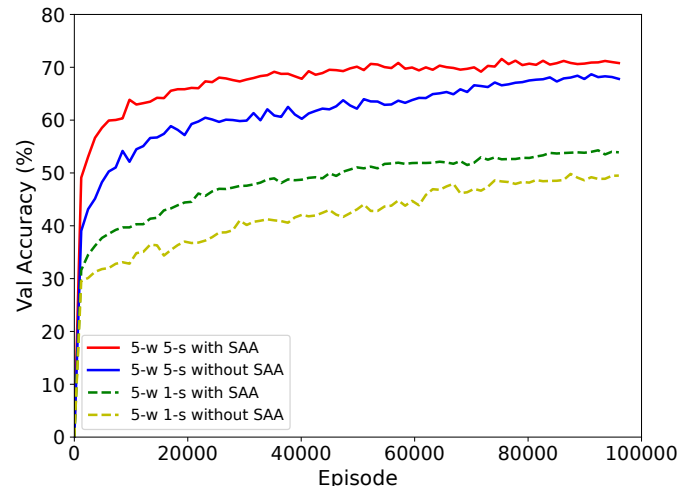


Fig. 6. The validation accuracy on the miniImageNet dataset.

TABLE III
ZERO-SHOT CLASSIFICATION ACCURACIES ON THE CUB DATASET AND THE SUN DATASET. “~” MEANS “NO REPORTED”.

Model	CUB	SUN
ALE [35]	26.9	~
ESZSL [39]	~	65.8
SSE [62]	30.4	82.5
SC [63]	44.3	~
LATEM [64]	45.5	~
SJE [36]	50.1	~
DS-SJE [41]	50.4	~
AS-SJE [41]	50.9	~
PN [20]	54.6	85.8
Our Method	57.8	88.6

2) *Zero-shot Classification*: In zero-shot classification, we also evaluate our proposed approach on the prototypical network. Table III shows the comparison between the improved version and other existing methods which have evaluation records in the same setting.

Like in few-shot classification experiments, there is no data augmentation involved during training and all the methods in the table are inductive methods.

The results show that our proposed approach in zero-shot classification achieves a significant performance boost compared with other existing methods. It further demonstrates the effectiveness of introducing semantic alignment to the network in zero-shot classification.

E. Ablation Study

We study the impacts of sub-modules, the manually-set margin α in $loss_w$, the hyper-parameter λ in $loss$ and the dimension of the label embeddings. Experiments are conducted on the miniImageNet dataset.

1) *Impacts of sub-modules*: The semantic-aligned attention mechanism consists of two sub-modules and we study their impacts on the preformance, as shown in Table IV. Here “AM” refers to the attention mechanism in Section and “SM” refers to the semantic-aligned mechanism described in Section III-B. Additionally, “(1)” means each convolutional block in the network contains both the attention mechanism and the semantic-aligned mechanism. “(2)” means only the last convolutional blocks contain both mechanisms while the first three convolutional blocks only have the attention mechanism, which is used in our network described in Section III-C.

The first thing we could see is that our semantic-aligned attention mechanism, the combination of the attention mechanism and the semantic-aligned mechanism surpasses the

attention mechanism or the semantic-aligned mechanism alone in improving feature embedding of the prototypical network. The attention mechanism alone improves both the 5-way 1-shot and the 5-way 5-shot performances by 2.14% and 1.28% respectively. It indicates the importance of local features in forming accurate class embeddings. The semantic-aligned mechanism alone, however, deteriorates the model. We believe this is because it is more difficult to learn the relationship between the semantic description of the object and the global visual features. With the semantic-aligned attention mechanism, the local visual features are generated so that visual-semantic alignment can be well learnt to refine local feature embedding. In this case, both the 5-way 1-shot and the 5-way 5-shot performances are improved compared with the network with the attention mechanism alone. Therefore, our semantic-aligned attention mechanism is more effective in feature embedding.

The second thing we could obverse is that introducing semantic alignment into the last layer alone is better than into every single layer of the network. As a matter of fact, many works related to visual-semantic embedding applies semantic alignment in the last layer. It verifies the effectiveness of our network architecture selection in Section 3.3.

2) *Impacts of α* : α is a hyper-parameter in computing $loss_w$ in the network, so we study the impact of its value on few-shot classification on the miniImageNet dataset, as shown in Fig. 7. It is easy to observe that the 5-way 1-shot performance is best when α is set to be 0.3 and the optimal α is 0.4 in the 5-way 5-shot performance. We set the hyper-parameter α according to this in our experiments.

As a matter of fact, α controls the margin in exploring the relationship between visual local regions and class label embeddings in a common embedding space. A higher margin might lead to the overfitting problem. This is why there is a performance degradation when α becomes bigger.

3) *Impacts of λ* : λ is a hyper-parameter in calculating $loss$ in the overall network, and we study its impact on few-shot classification on the miniImageNet dataset, as shown in Fig. 8. It can be observed that the optimal value of λ is within the range of 0.6 to 1.2 under the both circumstances of 5-way 1-shot and 5-way 5-shot.

In fact, λ can be seen as a coefficient controlling the role the semantic-aligned mechanism plays in updating the network. We choose 1.0 in our experiments.

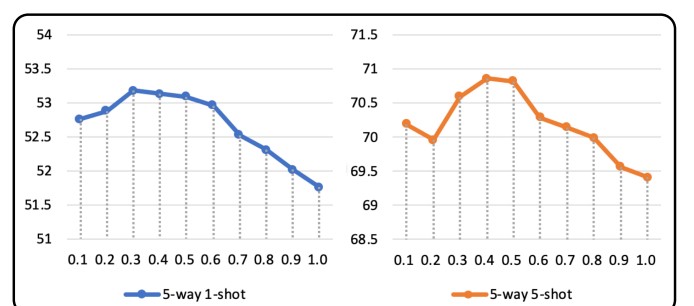


Fig. 7. The impact of α in computing $loss_w$ on few-shot classification on the miniImageNet dataset.

TABLE IV
ABLATION STUDY RESULTS ON THE MINIIMAGENET DATASET.

Model	5-way 1-shot	5-way 5-shot
ProtoNet	49.42	68.20
ProtoNet+AM	51.56	69.48
ProtoNet+SM	47.87	67.12
ProtoNet+SAA ⁽¹⁾	52.79	70.54
ProtoNet+SAA ⁽²⁾	53.18	70.86

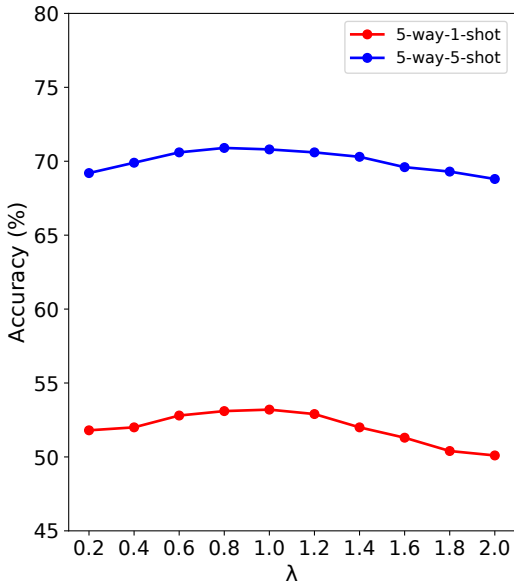


Fig. 8. The impact of λ in computing the overall network loss on few-shot classification on the miniImageNet dataset.

4) *Impacts of the dimension of the label embeddings:* The pre-trained word embedding model *GloVe* [27] offers three kinds of word embeddings in three different dimensions: 100, 200 and 300. A higher dimension means richer prior semantic knowledge in the word embeddings. We study the impact of the dimension of the label embeddings in our method on few-shot classification in Fig. 9.

When the dimension becomes bigger, our method performs better in few-shot classification under both circumstances of 5-way 1-shot and 5-way 5-shot. We choose 300 as the dimension of the label embeddings in our experiments.

F. Visualization

Visualization of feature embedding in Fig. 10 using t-SNE [65] perfectly proves the effectiveness of our proposed SAA

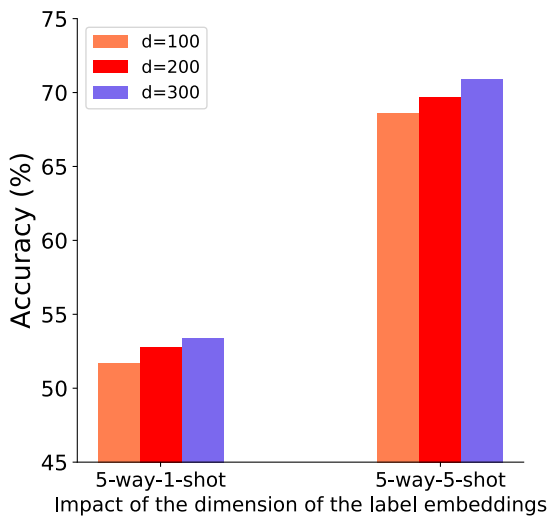


Fig. 9. The impact of the dimension of the label embeddings on few-shot classification on the miniImageNet dataset.

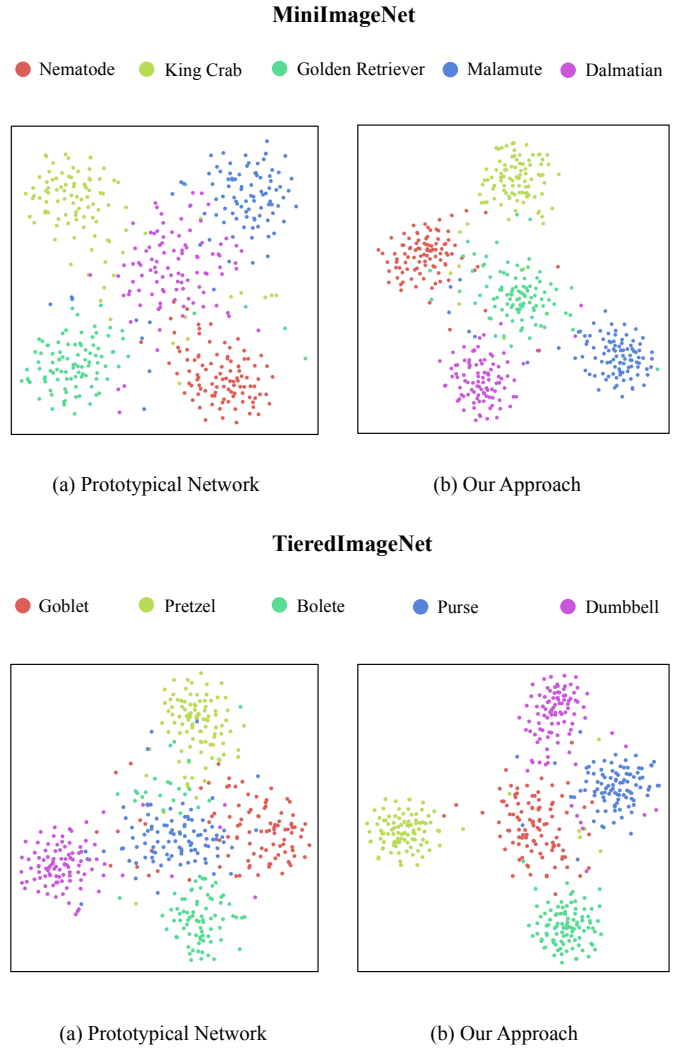


Fig. 10. The t-SNE visualization of feature embedding on the miniImageNet dataset and the tieredImageNet dataset. It is under the 5-way 5-shot setting and 100 support samples are included in each class for a better view. We can see that the effect of introducing semantic-aligned attention mechanism to feature embedding is obvious: making clusters more compact and discriminative from each other.

approach.

As shown in Fig. 10, the features are computed under the 5-way 5-shot setting. The 5 classes selected from the miniImageNet test dataset are “Nematode”, “King Crab”, “Golden Retriever”, “Malamute” and “Dalmatian”. The 5 classes selected from the tieredImageNet test dataset are “Goblet”, “Pretzel”, “Bolete”, “Purse” and “Dumbbell”. To have a better view, 100 support samples are visualized for each class. Fig. 10(a) corresponds to the prototypical network and Fig. 10(b) corresponds to the improved version with our proposed semantic-aligned attention mechanism. As can be seen clearly, the improved version of the prototypical network with SAA has more compact clusters and features in one class are discriminative from ones in other classes. It indicates that our proposed SAA helps find intra-class commonality and improves feature embedding greatly in the model.

We also visualize the class activation maps and compare them in two networks, one is ours with SAA and the other

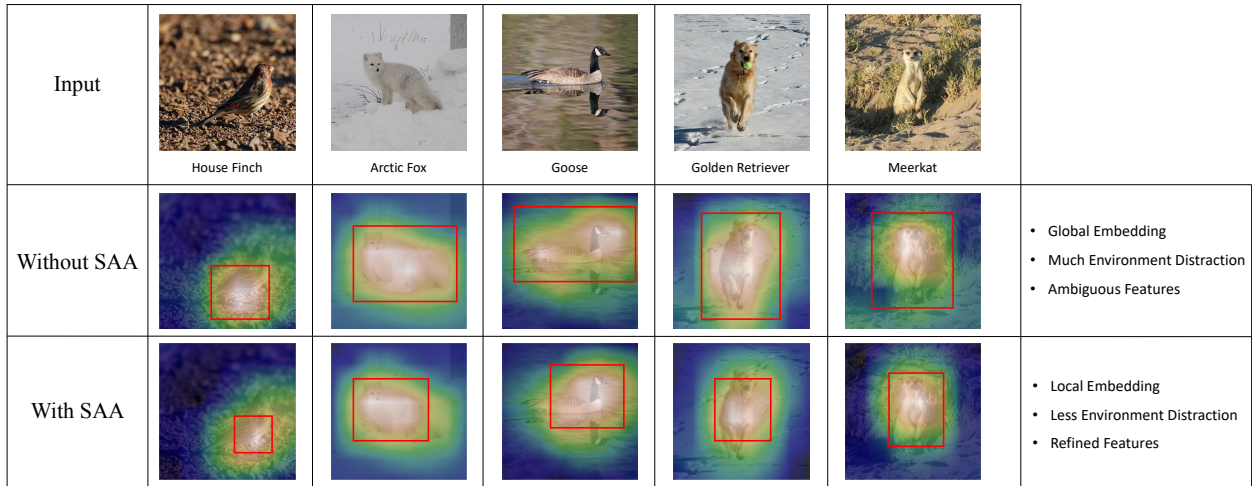


Fig. 11. Visualization of class activation maps on few-shot classification. Images in the first row are inputs selected from the miniImageNet dataset. The class activation maps are blended with the original images for a better view. The second row shows the ones generated from the network without SAA. The third row shows the ones generated from our method. It is easy to see that our method offers a refined attentive map.

is without SAA, as shown in Fig. 11. Our method generates refined attentive class activation maps not easily affected by the background. In other words, the network can focus on the pivotal local information and alleviate noisy global distraction. It further explains why the class embedding is better generated in our method.

V. CONCLUSION

In this paper, we introduced a Semantic-Aligned Attention (SAA) mechanism for few-shot classification that can improve feature embedding in most embedding and metric-learning approaches like the prototypical network. To be more specific, the mechanism highlights pivotal local information with attention mechanism and refines extracted local features with semantic alignment. We further extended the idea to zero-shot classification by introducing important semantic information in generating the class embedding. Extensive experimental results show that our approach in few-shot classification lifts the performance on the miniImageNet dataset and the tiered-ImageNet dataset and our approach in zero-shot classification boosts the performance on the CUB dataset and the SUN dataset. The t-SNE visualization shows more compact and discriminative clusters in our method and the class activation map visualization shows a refined attentive map offered by our method. They further verify the effectiveness of our proposed approach.

ACKNOWLEDGMENT

This work was supported in part by the National Natural Science Foundation of China under grants (No. 61976049 and No. 61632007); the Fundamental Research Funds for the Central Universities under Project (No. ZYGX2019Z015) and the Sichuan Science and Technology Program, China (No. 2019ZDZX0008, No. 2020YFS0057 and No. 2019YFG003).

REFERENCES

- [1] K. He, X. Zhang, S. Ren, and J. Sun, “Deep residual learning for image recognition,” in *Proceedings of the IEEE conference on computer vision and pattern recognition*, 2016, pp. 770–778.
- [2] A. Krizhevsky, I. Sutskever, and G. E. Hinton, “Imagenet classification with deep convolutional neural networks,” in *Advances in neural information processing systems*, 2012, pp. 1097–1105.
- [3] C. Szegedy, W. Liu, Y. Jia, P. Sermanet, S. Reed, D. Anguelov, D. Erhan, V. Vanhoucke, and A. Rabinovich, “Going deeper with convolutions,” in *Proceedings of the IEEE conference on computer vision and pattern recognition*, 2015, pp. 1–9.
- [4] J. Deng, W. Dong, R. Socher, L.-J. Li, K. Li, and L. Fei-Fei, “Imagenet: A large-scale hierarchical image database,” in *2009 IEEE conference on computer vision and pattern recognition*. Ieee, 2009, pp. 248–255.
- [5] L. Fei-Fei, R. Fergus, and P. Perona, “One-shot learning of object categories,” *IEEE transactions on pattern analysis and machine intelligence*, vol. 28, no. 4, pp. 594–611, 2006.
- [6] Z. Chen, Y. Fu, K. Chen, and Y.-G. Jiang, “Image block augmentation for one-shot learning,” in *Proceedings of the AAAI Conference on Artificial Intelligence*, vol. 33, 2019, pp. 3379–3386.
- [7] Z. Chen, Y. Fu, Y.-X. Wang, L. Ma, W. Liu, and M. Hebert, “Image deformation meta-networks for one-shot learning,” in *Proceedings of the IEEE Conference on Computer Vision and Pattern Recognition*, 2019, pp. 8680–8689.
- [8] B. Hariharan and R. Girshick, “Low-shot visual recognition by shrinking and hallucinating features,” in *Proceedings of the IEEE International Conference on Computer Vision*, 2017, pp. 3018–3027.
- [9] E. Schwartz, L. Karlinsky, J. Shtok, S. Harary, M. Marder, A. Kumar, R. Feris, R. Giryes, and A. Bronstein, “Delta-encoder: an effective sample synthesis method for few-shot object recognition,” in *Advances in Neural Information Processing Systems*, 2018, pp. 2845–2855.
- [10] S. Tsutsui, Y. Fu, and D. Crandall, “Meta-reinforced synthetic data for one-shot fine-grained visual recognition,” in *Advances in Neural Information Processing Systems*, 2019, pp. 3057–3066.
- [11] C. Finn, P. Abbeel, and S. Levine, “Model-agnostic meta-learning for fast adaptation of deep networks,” in *Proceedings of the 34th International Conference on Machine Learning-Volume 70*. JMLR.org, 2017, pp. 1126–1135.
- [12] M. A. Jamal and G.-J. Qi, “Task agnostic meta-learning for few-shot learning,” in *Proceedings of the IEEE Conference on Computer Vision and Pattern Recognition*, 2019, pp. 11719–11727.
- [13] Z. Li, F. Zhou, F. Chen, and H. Li, “Meta-sgd: Learning to learn quickly for few-shot learning,” *arXiv preprint arXiv:1707.09835*, 2017.
- [14] N. Mishra, M. Rohaninejad, X. Chen, and P. Abbeel, “A simple neural attentive meta-learner,” *arXiv preprint arXiv:1707.03141*, 2017.
- [15] A. Nichol, J. Achiam, and J. Schulman, “On first-order meta-learning algorithms,” *arXiv preprint arXiv:1803.02999*, 2018.
- [16] S. Ravi and H. Larochelle, “Optimization as a model for few-shot learning,” 2016.

- [17] Q. Sun, Y. Liu, T.-S. Chua, and B. Schiele, "Meta-transfer learning for few-shot learning," in *Proceedings of the IEEE Conference on Computer Vision and Pattern Recognition*, 2019, pp. 403–412.
- [18] H. Li, D. Eigen, S. Dodge, M. Zeiler, and X. Wang, "Finding task-relevant features for few-shot learning by category traversal," in *Proceedings of the IEEE Conference on Computer Vision and Pattern Recognition*, 2019, pp. 1–10.
- [19] B. Oreshkin, P. R. López, and A. Lacoste, "Tadam: Task dependent adaptive metric for improved few-shot learning," in *Advances in Neural Information Processing Systems*, 2018, pp. 721–731.
- [20] J. Snell, K. Swersky, and R. Zemel, "Prototypical networks for few-shot learning," in *Advances in neural information processing systems*, 2017, pp. 4077–4087.
- [21] F. Sung, Y. Yang, L. Zhang, T. Xiang, P. H. Torr, and T. M. Hospedales, "Learning to compare: Relation network for few-shot learning," in *Proceedings of the IEEE Conference on Computer Vision and Pattern Recognition*, 2018, pp. 1199–1208.
- [22] O. Vinyals, C. Blundell, T. Lillicrap, D. Wierstra *et al.*, "Matching networks for one shot learning," in *Advances in neural information processing systems*, 2016, pp. 3630–3638.
- [23] H.-J. Ye, H. Hu, D.-C. Zhan, and F. Sha, "Learning embedding adaptation for few-shot learning," *arXiv preprint arXiv:1812.03664*, 2018.
- [24] S. Yan, S. Zhang, X. He *et al.*, "A dual attention network with semantic embedding for few-shot learning," in *Proceedings of the AAAI Conference on Artificial Intelligence*, vol. 33, 2019, pp. 9079–9086.
- [25] H. Xu, G. Qi, J. Li, M. Wang, K. Xu, and H. Gao, "Fine-grained image classification by visual-semantic embedding," in *IJCAI*, 2018, pp. 1043–1049.
- [26] B. Wang, Y. Yang, X. Xu, A. Hanjalic, and H. T. Shen, "Adversarial cross-modal retrieval," in *Proceedings of the 2017 ACM on Multimedia Conference*, 2017, pp. 154–162.
- [27] J. Pennington, R. Socher, and C. D. Manning, "Glove: Global vectors for word representation," in *Proceedings of the 2014 conference on empirical methods in natural language processing (EMNLP)*, 2014, pp. 1532–1543.
- [28] Z. Ji, Y. Fu, J. Guo, Y. Pang, Z. M. Zhang *et al.*, "Stacked semantics-guided attention model for fine-grained zero-shot learning," in *Advances in Neural Information Processing Systems*, 2018, pp. 5995–6004.
- [29] H. T. Shen, L. Liu, Y. Yang, X. Xu, Z. Huang, F. Shen, and R. Hong, "Exploiting subspace relation in semantic labels for cross-modal hashing," *IEEE Transactions on Knowledge and Data Engineering*, p. 10.1109/TKDE.2020.2970050, 2020.
- [30] T. Gao, X. Han, Z. Liu, and M. Sun, "Hybrid attention-based prototypical networks for noisy few-shot relation classification," in *Proceedings of the AAAI Conference on Artificial Intelligence*, vol. 33, 2019, pp. 6407–6414.
- [31] F. Hao, F. He, J. Cheng, L. Wang, J. Cao, and D. Tao, "Collect and select: Semantic alignment metric learning for few-shot learning," in *Proceedings of the IEEE International Conference on Computer Vision*, 2019, pp. 8460–8469.
- [32] R. Hou, H. Chang, M. Bingpeng, S. Shan, and X. Chen, "Cross attention network for few-shot classification," in *Advances in Neural Information Processing Systems*, 2019, pp. 4005–4016.
- [33] M. Ren, R. Liao, E. Fetaya, and R. Zemel, "Incremental few-shot learning with attention attractor networks," in *Advances in Neural Information Processing Systems*, 2019, pp. 5276–5286.
- [34] Z. Wu, Y. Li, L. Guo, and K. Jia, "Parn: Position-aware relation networks for few-shot learning," in *Proceedings of the IEEE International Conference on Computer Vision*, 2019, pp. 6659–6667.
- [35] Z. Akata, F. Perronnin, Z. Harchaoui, and C. Schmid, "Label-embedding for attribute-based classification," in *Proceedings of the IEEE Conference on Computer Vision and Pattern Recognition*, 2013, pp. 819–826.
- [36] Z. Akata, S. Reed, D. Walter, H. Lee, and B. Schiele, "Evaluation of output embeddings for fine-grained image classification," in *Proceedings of the IEEE Conference on Computer Vision and Pattern Recognition*, 2015, pp. 2927–2936.
- [37] M. Bucher, S. Herbin, and F. Jurie, "Improving semantic embedding consistency by metric learning for zero-shot classification," in *European Conference on Computer Vision*. Springer, 2016, pp. 730–746.
- [38] A. Frome, G. S. Corrado, J. Shlens, S. Bengio, J. Dean, M. Ranzato, and T. Mikolov, "Devise: A deep visual-semantic embedding model," in *Advances in neural information processing systems*, 2013, pp. 2121–2129.
- [39] B. Romera-Paredes and P. Torr, "An embarrassingly simple approach to zero-shot learning," in *International Conference on Machine Learning*, 2015, pp. 2152–2161.
- [40] Y. Liu, J. Guo, D. Cai, and X. He, "Attribute attention for semantic disambiguation in zero-shot learning," in *Proceedings of the IEEE International Conference on Computer Vision*, 2019, pp. 6698–6707.
- [41] S. Reed, Z. Akata, H. Lee, and B. Schiele, "Learning deep representations of fine-grained visual descriptions," in *Proceedings of the IEEE Conference on Computer Vision and Pattern Recognition*, 2016, pp. 49–58.
- [42] F. Shen, X. Zhou, J. Yu, Y. Yang, L. Liu, and H. T. Shen, "Scalable zero-shot learning via binary visual-semantic embeddings," *IEEE Transactions on Image Processing*, vol. 28, no. 7, pp. 3662–3674, 2019.
- [43] X. Xu, H. Lu, J. Song, Y. Yang, H. T. Shen, and X. Li, "Ternary adversarial networks with self-supervision for zero-shot cross-modal retrieval," vol. 50, no. 6, pp. 2400–2413, 2020.
- [44] R. Socher, M. Ganjoo, C. D. Manning, and A. Ng, "Zero-shot learning through cross-modal transfer," in *Advances in neural information processing systems*, 2013, pp. 935–943.
- [45] L. Zhang, T. Xiang, and S. Gong, "Learning a deep embedding model for zero-shot learning," in *Proceedings of the IEEE Conference on Computer Vision and Pattern Recognition*, 2017, pp. 2021–2030.
- [46] S. Woo, J. Park, J.-Y. Lee, and I. So Kweon, "Cbam: Convolutional block attention module," in *Proceedings of the European Conference on Computer Vision (ECCV)*, 2018, pp. 3–19.
- [47] S. Zagoruyko and N. Komodakis, "Paying more attention to attention: Improving the performance of convolutional neural networks via attention transfer," *arXiv preprint arXiv:1612.03928*, 2016.
- [48] U. Seiffert, "Multiple layer perceptron training using genetic algorithms," in *ESAN*. Citeseer, 2001, pp. 159–164.
- [49] D. J. Finney, *Probit analysis: a statistical treatment of the sigmoid response curve*. Cambridge university press, cambridge, 1952.
- [50] J. Weston, S. Bengio, and N. Usunier, "Large scale image annotation: learning to rank with joint word-image embeddings," *Machine learning*, vol. 81, no. 1, pp. 21–35, 2010.
- [51] M. Ren, E. Triantafillou, S. Ravi, J. Snell, K. Swersky, J. B. Tenenbaum, H. Larochelle, and R. S. Zemel, "Meta-learning for semi-supervised few-shot classification," *arXiv preprint arXiv:1803.00676*, 2018.
- [52] C. Wah, S. Branson, P. Welinder, P. Perona, and S. Belongie, "The caltech-ucsd birds-200-2011 dataset," 2011.
- [53] G. Patterson and J. Hays, "Sun attribute database: Discovering, annotating, and recognizing scene attributes," in *2012 IEEE Conference on Computer Vision and Pattern Recognition*. IEEE, 2012, pp. 2751–2758.
- [54] A. Paszke, S. Gross, S. Chintala, and G. Chanan, "Pytorch: Tensors and dynamic neural networks in python with strong gpu acceleration," *PyTorch: Tensors and dynamic neural networks in Python with strong GPU acceleration*, vol. 6, 2017.
- [55] O. Russakovsky, J. Deng, H. Su, J. Krause, S. Satheesh, S. Ma, Z. Huang, A. Karpathy, A. Khosla, M. Bernstein *et al.*, "Imagenet large scale visual recognition challenge," *International journal of computer vision*, vol. 115, no. 3, pp. 211–252, 2015.
- [56] C. H. Lampert, H. Nickisch, and S. Harmeling, "Attribute-based classification for zero-shot visual object categorization," *IEEE transactions on pattern analysis and machine intelligence*, vol. 36, no. 3, pp. 453–465, 2013.
- [57] D. P. Kingma and J. Ba, "Adam: A method for stochastic optimization," *arXiv preprint arXiv:1412.6980*, 2014.
- [58] T. Munkhdalai and H. Yu, "Meta networks," in *Proceedings of the 34th International Conference on Machine Learning-Volume 70*. JMLR.org, 2017, pp. 2554–2563.
- [59] Q. Cai, Y. Pan, T. Yao, C. Yan, and T. Mei, "Memory matching networks for one-shot image recognition," in *Proceedings of the IEEE conference on computer vision and pattern recognition*, 2018, pp. 4080–4088.
- [60] A. Antoniou, H. Edwards, and A. Storkey, "How to train your maml," 2018.
- [61] C. Simon, P. Koniusz, and M. Harandi, "Projective subspace networks for few-shot learning," 2018.
- [62] Z. Zhang and V. Saligrama, "Zero-shot learning via semantic similarity embedding," in *Proceedings of the IEEE international conference on computer vision*, 2015, pp. 4166–4174.
- [63] R. Liao, A. Schwing, R. Zemel, and R. Urtasun, "Learning deep parsimonious representations," in *Advances in Neural Information Processing Systems*, 2016, pp. 5076–5084.
- [64] Y. Xian, Z. Akata, G. Sharma, Q. Nguyen, M. Hein, and B. Schiele, "Latent embeddings for zero-shot classification," in *Proceedings of the IEEE Conference on Computer Vision and Pattern Recognition*, 2016, pp. 69–77.
- [65] L. v. d. Maaten and G. Hinton, "Visualizing data using t-sne," *Journal of machine learning research*, vol. 9, no. Nov, pp. 2579–2605, 2008.